## Title

Detecting DNA and RNA and Differentiating Single-Nucleotide Variations via Field-Effect Transistors



## Journal

Nano Letters, 20(8)

## ISSN

1530-6984

## Authors

Cheung, Kevin M
Abendroth, John M
Nakatsuka, Nako
et al.

## Publication Date

2020-08-12

## DOI

10.1021/acs.nanolett.0c01971

Peer reviewed

HHS Public Access

Author manuscript

*Nano Lett*. Author manuscript; available in PMC 2020 August 20.

Published in final edited form as:

*Nano Lett*. 2020 August 12; 20(8): 5982–5990. doi:10.1021/acs.nanolett.0c01971.

# Detecting DNA and RNA and Differentiating Single-Nucleotide Variations *via* Field-Effect Transistors

**Kevin M. Cheung**[1,2], **John M. Abendroth**[1,2], **Nako Nakatsuka**[1,2], **Bowen Zhu**[2,3], **Yang Yang**[2,3], **Anne M. Andrews**[1,2,4,*], **Paul S. Weiss**[1,2,3,5,*]

[1]Department of Chemistry and Biochemistry, University of California, Los Angeles, Los Angeles, California 90095, United States

[2]California NanoSystems Institute, University of California, Los Angeles, Los Angeles, California 90095, United States

[3]Department of Materials Science and Engineering, University of California, Los Angeles, Los Angeles, California 90095, United States

[4]Department of Psychiatry and Biobehavioral Sciences, Semel Institute for Neuroscience & Human Behavior, and Hatos Center for Neuropharmacology, University of California, Los Angeles, Los Angeles, California 90095, United States

[5]Department of Bioengineering, University of California, Los Angeles, Los Angeles, California 90095, United States

## Abstract

We detect short oligonucleotides and distinguish between sequences that differ by a single base, using label-free, electronic field-effect transistors (FETs). Our sensing platform utilizes ultrathin film indium-oxide FETs chemically functionalized with single-stranded DNA (ssDNA). The ssDNA-functionalized semiconducting channels in FETs detect fully complementary DNA sequences and differentiate these sequences from those having different types and locations of single base-pair mismatches. Changes in charge associated with surface-bound ssDNA *vs.* double-stranded DNA (dsDNA) alter FET channel conductance to enable detection due to differences in DNA duplex stability. We illustrate the capability of ssDNA-FETs to detect complementary RNA sequences and to distinguish from RNA sequences with single nucleotide variations. The development and implementation of electronic biosensors that rapidly and sensitively detect and differentiate oligonucleotides present new opportunities in the fields of disease diagnostics and precision medicine.

[*]To whom correspondence should be addressed: psw@cnsi.ucla.edu, aandrews@mednet.ucla.edu.

Author Contributions

All authors designed the experiments. KMC, JMA, NN, and BZ carried out the experiments. All authors performed data analysis and interpreted the results. KMC, AMA, and PSW wrote the manuscript with input from all authors.

Supporting Information

Experimental methods and a FET concentration experiment, time responses, I-V curves, non-complementary controls, DNA melt curves, rinse experiment, and statistical methods and table. The Supporting Information is available free of charge on the ACS Publications website at DOI: https://doi.org/10.1021/acs.nanolett.0c01971

KMC, AMA, and PSW have filed an international patent application on detecting and discriminating nucleic acid sequences using FETs, International application PCT/US2019/027080.

## Graphical Abstract

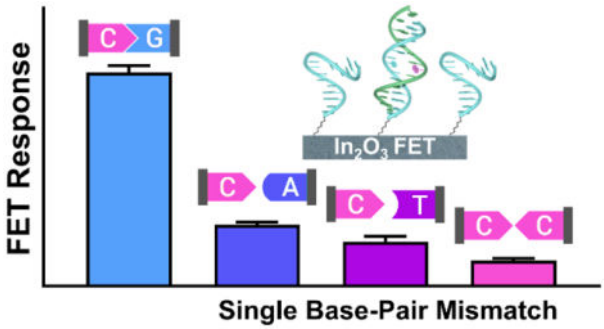


### Keywords

DNA; RNA; mismatch; polymorphism; SNP; SNV; FET; sensing; biosensor

Nucleic acid diagnostics have enabled many opportunities in modern medicine for the analysis, diagnosis, and treatment of genetic and infectious diseases.[1] The identification and subsequent detection of disease associated nucleic acids is necessary for personalized and preventative medicine.[1] Moreover, the recent global pandemic of 2019 novel coronavirus (COVID-19) illustrates the unmet need for rapid, flexible nucleic acid testing technology for disease diagnostics that is easily depolayble, manufacturable, and adaptable to new infectious agents once novel genomes are sequenced and identified.[2,3]

Single-nucleotide variations (SNVs) are important in both genomes and somatic mutations, such as in tumors, as they affect disease progression and therapeutic responses.[4] Thus, significant interest and efforts are aimed at identifying common and rare SNVs, their patterns of occurrence and relationships with complex diseases and biological traits. Detecting specific oligonucleotides and their variants rapidly in human populations and patient tissue samples will improve disease diagnostics and precision medicine.[4–8] The identification of known variants and the discovery and association of new variants with disease are both important.[1]

Single-nucleotide polymorphisms (SNPs) are the most common form of genetic variation typically defined as SNVs occurring in at least 1% of the population.[4–8] On average, SNPs occur every 1000 nucleotides in human genomes and contribute to individuality in humans and other organisms.[4–10] Single-nucleotide polymorphisms are found in coding and noncoding regions of DNA, and in RNA (*e.g.*, mRNA, tRNA, miRNA).[11–16] Many SNPs have no discernable effects on health or development. Nonetheless, SNPs have been correlated with genetic susceptibility to asthma,[17] Alzheimer's disease,[18] β-thalassemia,[19] sickle cell disease,[20] and cancers,[14,21–24] as well as responses to xenobiotics.[5,25]

Commonly, SNVs are identified and profiled using techniques that require oligonucleotide amplification (*i.e.*, polymerase chain reaction, PCR)[4] and/or fluorophore-labeled oligonucleotides (*e.g.*, molecular beacons, DNA microarrays).[4,26,27] These methods are powerful in laboratory settings, yet are limited in terms of translation to clinical diagnostic

and point-of-care applications. Electrochemical detection,[28] nanopore sequencing,[29] mass spectrometry,[19,30] and high-performance liquid chromatography[31] show promise for SNV detection. These techniques suffer from throughput issues, are complex, expensive, and labor intensive, and often require nucleotide labeling and/or amplification.

Applications that necessitate analyzing large numbers of patient DNA or RNA samples, or multiple SNVs, highlight the benefits of developing sensor platforms capable of rapid, direct, multiplexed, and label-free SNV detection and read-out. Field-effect transistor (FET) -based biosensors have been used to identify and to quantify biological analytes wherein target binding is directly transduced into changes in FET conductance (electronic signals) for high-sensitivity detection.[32–40] Transistor surfaces are modified with receptors (*e.g.*, proteins, antibodies, nucleic acids) to enable selective molecular recognition of a variety of targets ranging from small molecules[32,33,40] to nucleic acids[41,42] and proteins.[43–45]

We present a strategy for detecting oligonucleotide sequences and SNVs using ultrathin-film quasi-2D metal-oxide FETs. We have demonstrated the use of this type of FET for the sensitive and selective detection of a range of small molecules (*e.g.*, neurotransmitters, amino acids, sugars, and lipids) in complex biological fluids.[32,33,40] We functionalize the semiconductor channel material of FETs with ssDNA to detect complementary DNA hybridization. We distinguish FET responses associated with single base-pair mismatches of different types and positions to illustrate the potential for SNV genotyping. We hypothesize that sequence differentiation is contingent upon differences in duplex stability, and thus the degree of DNA hybridization (*i.e.*, surface density of dsDNA *vs* ssDNA). We illustrate RNA detection and sequence differentiation at the single-base level. The capability to discriminate oligonucleotides that differ by a single base using thin-film metal oxide FETs is anticipated to enable the development of parallelized electronic arrays for rapid SNP genotyping and tissue or cellular transcriptomics.[46]

A representative FET with the detection set-up is shown in Figure 1A. Arrays of transistors were fabricated with ultrathin $In_2O_3$ (*ca.* 4 nm) deposited as the channel material using a high-throughput solution-processable sol-gel method.[32,33,40,47,48] Thiolated ssDNA (probe) was functionalized on FET surfaces *via* attachment to self-assembled silanes on the indium oxide channels using an amine-thiol linker (Figure 1B).[32,33] Individual ssDNA-functionalized FETs were exposed to solutions containing oligonucleotides (targets) and FET responses were measured over a period of 30 min (*vide infra*). Device responses were determined after exposure to targets that were non-complementary, fully complementary, or had single base-pair mismatches with respect to the probe sequences functionalized on FET surfaces (Figure 1C).

We exposed FETs to complementary *vs.* non-complementary DNA (Figure 2A). Calibrated responses were determined by dividing baseline subtracted current responses by the change in source-drain current with the voltage sweep to minimize device-to-device variation (see Supplemental Methods).[49] The FETs incubated with target oligonucleotides complementary to ssDNA probe sequences on the $In_2O_3$ channel surfaces showed initial increases in conductance that stabilized over 30 min (Figure 2B). By contrast, FETs incubated with a non-complementary sequence showed an initial increase that returned to near baseline over

time. We attribute divergent behavior following response stabilization to differences in DNA hybridization. In the case of fully complementary target DNA, hybridization produced increases in stabilized FET calibrated responses over a range of target concentrations (Figure S1), whereas a lack of hybridization for non-complementary sequences resulted in minimal conductance change after stabilization (*e.g.*, 30 min) (Figure 2B).

Sensor responses were then determined after exposing ssDNA-functionalized FETs to DNA oligonucleotides with different single base-pair mismatches (*i.e.*, CA, CT, CC) at the 5$^{th}$ position distal to the thiolate attachment (Figure 3A). Target sequences were designed to be short (*i.e.*, 15-mers), as single base-pair mismatches are more destabilizing in shorter duplexes.[50] Similar to fully complementary and non-complementary responses, sensor responses associated with mismatched sequences stabilized after 20–30 min of incubation (Figure S2,3). Responses at 30-min post-DNA addition were averaged all measurements. In all cases, FETs exposed to mismatched DNA sequences had significantly lower calibrated responses compared to FETs exposed to fully complementary target DNA (Figure 3B). Thus, sensors distinguished DNA sequences that differed by a single base compared to the fully complementary sequence. Moreover, mean sensor responses for the various 5$^{th}$ position mismatches differed significantly from one another (Figure 3B), demonstrating that sensor responses discriminated sequences with different types of single base-pair mismatches.

In addition to DNA sequences with different types of single-base alterations at the *same* position, the responses of ssDNA-functionalized FETs to sequences with the same mismatch at *different* positions along the target strand were determined (Figure 3C). Time responses (Figure S4A,B) were comparable to those for mismatches involving different nucleotides at the same position and non-complementary DNA (Figure S2). Sensors exposed to targets with CC mismatches at the 5$^{th}$, 10$^{th}$, or 15$^{th}$ positions from the thiolate attachment showed greatly reduced responses compared to those of the analogous fully complementary sequence (Figure 3D). The ability to distinguish sequences that differ with respect to mismatch distance from FET surfaces illustrates that oligonucleotides that differ by as little as a single nucleotide, regardless of position, are differentiated from perfectly matched complementary sequences. Here again, minimal responses to non-complementary sequences were observed (Figure S4C,D).

The transfer characteristics (*I*-*V* curves) of ssDNA-FETs after incubation with complementary DNA showed reductions in current with respect to time (Figures S5A and S6A). Two competing effects associated with hybridization are hypothesized to contribute to changes in FET conductance. (1) Negative charge near FET surfaces *increases* after duplex formation because one negative charge is added per base in the hybridized strand. (2) By contrast, negative charge near FET surfaces *decreases* after duplex formation due to the increased stiffness of double-stranded *vs* single-stranded DNA. Hybridization increases the radius of gyration of DNA (*i.e.*, DNA is extended from *ca.* 1.5 nm for ssDNA to 5 nm for dsDNA for the sequences investigated).[51] We conclude the former effect dominates since the direction of change in FET conductance indicates a net increase in negative charge close to FET surfaces.

The transfer characteristics observed here are consistent with our previous findings showing that changes in FET transfer characteristics (*i.e.*, decreases in current) for *n*-type $In_2O_3$ semiconductor materials are predominantly due to gating (*i.e.*, band bending)[52] associated with negatively charged DNA backbones.[33,40] Moreover, as per our previous work with aptamer-based FET sensors, the directions of change of the *I-V* curves in Figures S5 and S6 indicate accumulation of net negative surface charge and electrostatic repulsion of semiconductor charge carriers, consistent with DNA hybridization. Unlike in one of our earlier studies in which ssDNA was inserted into defects in well-formed self-assembled alkanethiol monolayers on Au,[53] ssDNA functionalized *via* silane chemistry on semiconductor channels in FETs is likely to be disorganized and dsDNA may lay across surfaces, which would increase the gating effect associated with DNA hybridization.

A return to baseline was observed after initial current changes for non-complementary and mismatched DNA incubation (Figures S5B,C and S6B,C). Initial increases in FET calibrated responses (decreases in current) after DNA addition are due to the introduction of solutions containing negatively charged DNA near FET surfaces, as well as perturbation of FET surfaces due physically to mixing sample solutions during DNA addition. The return to baseline implies little to no hybridization (*i.e.*, minimal accumulation of negative charge near FET surfaces) for non-complementary and mismatched sequences with respect to time.

To investigate the contributions of duplex stability to DNA detection *via* ssDNA-FETs, DNA melt-curves were determined for sequences with mismatches at the $5^{th}$ position from the thiolate modification *vs* the fully complementary target (Figure 4A). The temperature at which dsDNA dehybridizes (*i.e.*, melts) is indicative of the stability of hybridized oligonucleotides; more stable duplexes have higher melting temperatures.[54–56] The melt-curves indicated that the duplex with the CC mismatch had the lowest melting temperature (*i.e.*, lowest stability), followed by the duplex with the CT mismatch, and then the CA mismatch. The melting temperature for the fully complementary duplex was ~10 °C higher than for the mismatched duplexes. Sequences with CC mismatches at different positions similiarly showed reduced melting temperatures compared to the fully complementary duplex (Figure S7).

The FET responses for various duplexes and the corresponding melting temperatures were highly correlated ($R^2$>0.99; Figure 4B) suggesting that FET responses are associated with the relative stabilities of the hybridized DNA sequences. These results are consistent with the hypothesis that DNA detection *via* ssDNA-FETs is based on dynamic equilibria wherein duplex stability is related to the probability of hybridization and thus, greater negative charge near FET surfaces. Mismatched DNA sequences, which are thermodynamically less stable (*i.e.*, have lower melting temperatures), are statistically less likely to be hybridized with surface-tethered ssDNA probes leading to attenuated accumulation of surface negative charge and lower measured FET responses. Rinsing of FET surfaces after 30 min of DNA incubation produced a decreased response for the non-complementary sequence *vs.* a minimal change for complementary and CC mismatched sequences (Figure S8), suggesting that small FET responses arising from non-complementary DNA are largely due to nonspecific adsorption.

To investigate whether our approach can be used to detect RNA, we tested ssDNA-functionalized thin-film $In_2O_3$ FETs with complementary, (CC) mismatched, and non-complementary RNA sequences (Figure 5A). Detection of RNA is important in testing for the presence of diseases, such as infection by RNA viruses.[3] Furthermore, single-nucleotide polymorphisms occur in RNA (*vide supra*), and similar to SNVs in DNA, have important implications in genetic diseases.[11–14] Genotyping SNVs in RNA could be advantageous for applications such as noninvasive prenatal diagnostics, where placental RNA can be obtained from maternal plasma samples.[12] Notably, DNA-RNA duplexes adopt an A-form helical conformation compared to the B-form helix typical of dsDNA.[57] Significant FET calibrated responses were observed only in the case of the fully complementary RNA sequence; mismatched and non-complementary sequences produced negligible changes in FET responses (Figure 5B).

In sum, we illustrate the use of a platform for electronic, sequence-specific detection of DNA and RNA. Oligonucleotides that differed by only a single base were readily distinguishable using solution processable ultrathin-film metal oxide FET sensors. The detection and discrimination of single base-pair mismatches in dsDNA and RNA-DNA duplexes illustrates the potential of this platform for label-free, electronic SNV genotyping. To detect specific SNVs, different FETs functionalized with different probe sequences would be fabricated in sensor arrays.[58] The fabrication methods used here are well suited to producing FET arrays.[32,40,47,59–61] Using two FETs as an example, one functionalized with ssDNA fully complementary to a SNV major allele and the other functionalized with ssDNA fully complementary to the corresponding minor allele, DNA (or RNA) samples from homozygous major or minor allele carriers or hemizygous individuals could be straightforwardly differentiated (*i.e.*, genotyped).

We posit that the mechanism of our ssDNA-FET platform is based on the detection of differences in nucleic acid hybridization near the surfaces of transistors. Based on this detection method, the platform is not limited to the sequences investigated here; we expect that any nucleic acid sequence and those with a variation, single nucleotide or otherwise, that results in reduced hybridization stability compared to the fully complementary sequence could be detected and discriminated.

Longer ssDNA sequences can be tethered to FET surfaces for the detection of multiple mismatches along the same sequence.[62] Additionally, modulating the ionic strength of the sensing solution changes the charge screening distance near FET semiconducting channels (*i.e.*, the Debye length), thus changing the (distance) range of sensitivity of the sensor.[33,40] The latter parameter suggests a strategy for screening SNVs that are closer to or further away from FET channels. Experiments comparing the gating associated with shorter complementary sequences *vs* longer complementary sequences will help to elucidate the contributions of charge *vs* change in radius of gyration to specific FET responses. Functionalizing arrays of FETs addressed with different ssDNA sequences that are perfect matches to different SNVs and their alleles will enable rapid profiling of DNA or RNA from tissues or cells, as well as detection of other types of nucleotide mutations (*e.g.*, using wild-card bases).[63]

Previously, FETs functionalized with ssDNA or sometimes, single-stranded peptide nucleic acids[64,65] have been used to detect DNA with specific sequences.[58,66–70] Such FET sensors have been demonstrated for real-time[65,71–73] and ultransensitive detection of DNA (*i.e.*, pico- to nanomolar detection limits).[66,70] Strategies employing FET sensors for the measurement of mismatched DNA sequences (*e.g.*, DNA strand displacement,[66] DNA nanotweezers[74]) have been developed towards electronic SNV detection.[64,75] Many FET platforms for DNA detection involve the use of one- or two-dimensional materials (*e.g.*, graphene,[41,45,66,72] graphene oxide,[73] carbon nanotubes,[35] semiconductor nanowires[76]) as channel materials. These materials maximize FET surface-to-volume ratios, presumably increasing device sensitivities. However, these materials entail challenges associated with synthesis, material heterogeneity, device reproducibility, and robust functionalization.[38,77,78]

Compared with other FET-based detection platforms, our functionalized transistors can be straightforwardly and reproducibly fabricated at the wafer scale in arrays using soft-lithographic techniques,[32,47,59–61,79,80] increasing the potential for rapid translation and deployment towards screening for pandemic infection, clinical disease diagnostics, and personalized healthcare applications.[81] In contrast to FETs based on 2D materials, solution processed ultrathin indium oxide films are highly uniform,[32,48,82] can be straightforwardly and selectively functionalized,[33,83] and have been demonstrated to have higher device sensitivities and lower detection limits in potentiometric biosensing applications (*e.g.*, pH and glucose sensing) compared with other 2D (*e.g.*, graphene, reduced graphene oxide, MoS2) and 1D (*e.g.*, carbon nanotubes, Si nanowires) materials.[48] Moreover, device architectures and performance can be tailored for specific applications (*i.e.*, nanostructuring),[32,47,84] and ssDNA surface densities can be altered to tune FET responses.[33] Ultimately, testing of clinical samples (*e.g.*, nasal swabs, serum, biobanked tissue samples) will be needed for platform validation. Even so, the ssDNA-FETs investigated here exemplify rapid, label-free, unamplified sequence-specific DNA and RNA detection with broad implications in screening and in precision medicine.

## Supplementary Material

Refer to Web version on PubMed Central for supplementary material.

## ACKNOWLEDGMENTS

This research was supported by funding from the National Institute on Drug Abuse (DA045550) and Nantworks. KMC thanks the Department of Chemistry and Biochemistry at UCLA for an SG fellowship. The authors thank Drs. Kayvan Niazi and Shahrooz Rabizadeh for inspiring and helpful discussions and Mr. Chuanzhen Zhao for assistance with FET fabrication. The table of contents image was made with graphics from biorender.com. The authors acknowledge the use of instruments at the UCLA-DOE Biochemistry Instrumentation Core Facility.

## REFERENCES

(1). Landegren U; Kaiser R; Caskey CT; Hood L DNA Diagnostics--Molecular Techniques and Automation. Science 1988, 242, 229–237. [PubMed: 3051381]

(2). Udugama B; Kadhiresan P; Kozlowski HN; Malekjahani A; Osborne M; Li VYC; Chen H; Mubareka S; Gubbay JB; Chan WCW Diagnosing COVID-19: The Disease and Tools for Detection. ACS Nano 2020, 14, 3822–3835.

(3). Wu F; Zhao S; Yu B; Chen Y-M; Wang W; Song Z-G; Hu Y; Tao Z-W; Tian J-H; Pei Y-Y; Yuan M-L; Zhang Y-L; Dai F-H; Liu Y; Wang Q-M; Zheng J-J; Xu L; Holmes EC; Zhang Y-Z A New Coronavirus Associated with Human Respiratory Disease in China. Nature 2020, 579, 265–269.

(4). Syvänen A-C Accessing Genetic Variation: Genotyping Single Nucleotide Polymorphisms. Nat. Rev. Genet 2001, 2, 930–942. [PubMed: 11733746]

(5). Schork NJ; Fallin D; Lanchbury JS Single Nucleotide Polymorphisms and the Future of Genetic Epidemiology. Clin. Genet 2000, 58, 250–264. [PubMed: 11076050]

(6). Cargill M; Altshuler D; Ireland J; Sklar P; Ardlie K; Patil N; Lane CR; Lim EP; Kalyanaraman N; Nemesh J; Ziaugra L; Friedland L; Rolfe A; Warrington J; Lipshutz R; Daley GQ; Lander ES Characterization of Single-Nucleotide Polymorphisms in Coding Regions of Human Genes. Nat. Genet 1999, 22, 231–238. [PubMed: 10391209]

(7). Wang DG; Fan J-B; Siao C-J; Berno A; Young P; Sapolsky R; Ghandour G; Perkins N; Winchester E; Spencer J; Kruglyak L; Stein L; Hsie L; Topaloglou T; Hubbell E; Robinson E; Mittmann M; Morris MS; Shen N; Kilburn D et al. Large-Scale Identification, Mapping, and Genotyping of Single-Nucleotide Polymorphisms in the Human Genome. Science 1998, 280, 1077–1082. [PubMed: 9582121]

(8). Sachidanandam R; Weissman D; Schmidt SC; Kakol JM; Stein LD; Marth G; Sherry S; Mullikin JC; Mortimore BJ; Willey DL; Hunt SE; Cole CG; Coggill PC; Rice CM; Ning Z; Rogers J; Bentley DR; Kwok P-Y; Mardis ER; Yeh RT et al. A Map of Human Genome Sequence Variation Containing 1.42 Million Single Nucleotide Polymorphisms. Nature 2001, 409, 928–933. [PubMed: 11237013]

(9). Wade CM; Daly MJ Genetic Variation in Laboratory Mice. Nat. Genet 2005, 37, 1175–1180. [PubMed: 16254563]

(10). Nishizaki SS; Boyle AP Mining the Unknown: Assigning Function to Noncoding Single Nucleotide Polymorphisms. Trends Genet. 2017, 33, 34–45. [PubMed: 27939749]

(11). Shen LX; Basilion JP; Stanton VP Single-Nucleotide Polymorphisms can Cause Different Structural Folds of mRNA. Proct. Natl. Acad. Sci. U. S. A 1999, 96, 7871–7876.

(12). Go ATJI; Visser A; Mulders MAM; Blankenstein MA; van Vugt JMG; Oudejans CBM 44 Single-Nucleotide Polymorphisms Expressed by Placental RNA: Assessment for Use in Noninvasive Prenatal Diagnosis of Trisomy 21. Clin. Chem 2007, 53, 2223–2224. [PubMed: 18267936]

(13). Duan R; Pak C; Jin P Single Nucleotide Polymorphism Associated with Mature miR-125a Alters the Processing of pri-miRNA. Hum. Mol. Genet 2007, 16, 1124–1131. [PubMed: 17400653]

(14). Jupe ER; Badgett AA; Neas BR; Craft MA; Mitchell DS; Resta R; Mulvihill JJ; Aston CE; Thompson LF Single Nucleotide Polymorphism in Prohibitin 3' Untranslated Region and Breast-Cancer Susceptibility. The Lancet 2001, 357, 1588–1589.

(15). Sun G; Yan J; Noltner K; Feng J; Li H; Sarkis DA; Sommer SS; Rossi JJ SNPs in Human miRNA Genes Affect Biogenesis and Function. RNA 2009, 15, 1640–1651. [PubMed: 19617315]

(16). Parisien M; Wang X; Pan T Diversity of Human tRNA Genes from the 1000-Genomes Project. RNA Biol. 2013, 10, 1853–1867. [PubMed: 24448271]

(17). Tantisira K; Klimecki WT; Lazarus R; Palmer LJ; Raby BA; Kwiatkowski DJ; Silverman E; Vercelli D; Martinez FD; Weiss ST Toll-Like Receptor 6 Gene (TLR6): Single-Nucleotide Polymorphism Frequencies and Preliminary Association with the Diagnosis of Asthma. Genes Immun. 2004, 5, 343–346. [PubMed: 15266299]

(18). Li H; Wetten S; Li L; Jean PL St.; Upmanyu R; Surh L; Hosford D; Barnes MR; Briley JD; Borrie M; Coletta N; Delisle R; Dhalla D; Ehm MG; Feldman HH; Fornazzari; Gauthier S; Goodgame N; Guzman D; Hammond S et al. Candidate Single-Nucleotide Polymorphisms From a Genomewide Association Study of Alzheimer Disease. JAMA Neurology 2008, 65, 45–53.

(19). Ding C; Chiu RWK; Lau TK; Leung TN; Chan LC; Chan AYY; Charoenkwan P; Ng ISL; Law H.-y.; Ma ESK; Xu X; Wanapirak C; Sanguansermsri; Liao C; Ai MATJ; Chui DHK; Cantor CR; Lo YMD MS Analysis of Single-Nucleotide Differences in Circulating Nucleic Acids: Application to Noninvasive Prenatal Diagnosis. Proc. Natl. Acad. Sci. U. S. A 2004, 101, 10762–10767. [PubMed: 15247415]

(20). Hoban MD; Cost GJ; Mendel MC; Romero Z; Kaufman ML; Joglekar AV; Ho M; Lumaquin D; Gray D; Lill GR; Cooper AR; Urbinati F; Senadheera S; Zhu A; Liu P-Q; Paschon DE; Zhang L; Rebar EJ; Wilber A; Wang X et al. Correction of the Sickle Cell Disease Mutation in Human Hematopoietic Stem/Progenitor Cells. Blood 2015, 125, 2597–2604. [PubMed: 25733580]

(21). Gail MH Discriminatory Accuracy From Single-Nucleotide Polymorphisms in Models to Predict Breast Cancer Risk. J. Natl. Cancer Inst 2008, 100, 1037–1041. [PubMed: 18612136]

(22). Manuguerra M; Saletta F; Karagas MR; Berwick M; Veglia F; Vineis P; Matullo G XRCC3 and XPD/ERCC2 Single Nucleotide Polymorphisms and the Risk of Cancer: A HuGE Review. Am. J. Epidemiol 2006, 164, 297–302. [PubMed: 16707649]

(23). Horikawa Y; Wood CG; Yang H; Zhao H; Ye Y; Gu J; Lin J; Habuchi T; Wu X Single Nucleotide Polymorphisms of microRNA Machinery Genes Modify the Risk of Renal Cell Carcinoma. Clin. Cancer. Res 2008, 14, 7956–7962. [PubMed: 19047128]

(24). Raghavan M; Lillington DM; Skoulakis S; Debernardi S; Chaplin T; Foot NJ; Lister TA; Young BD Genome-Wide Single Nucleotide Polymorphism Analysis Reveals Frequent Partial Uniparental Disomy Due to Somatic Recombination in Acute Myeloid Leukemias. Cancer Res. 2005, 65, 375–378. [PubMed: 15695375]

(25). Isla D; Sarries C; Rosell R; Alonso G; Domine M; Taron M; Lopez-Vivanco G; Camps C; Botia M; Nuñez L; Sanchez-Ronco M; Sanchez JJ; Lopez-Brea M; Barneto I; Paredes A; Medina B; Artal A; Lianes P Single Nucleotide Polymorphisms and Outcome in Docetaxel–Cisplatin-Treated Advanced Non-Small-Cell Lung Cancer. Ann. Oncol 2004, 15, 1194–1203. [PubMed: 15277258]

(26). Tyagi S; Kramer FR Molecular Beacons: Probes that Fluoresce upon Hybridization. Nat. Biotechnol 1996, 14, 303–308. [PubMed: 9630890]

(27). Zhang L; Wu C; Carta R; Zhao H Free Energy of DNA Duplex Formation on Short Oligonucleotide Microarrays. Nucleic Acids Res. 2006, 35, e18. [PubMed: 17169993]

(28). Xiao Y; Lou X; Uzawa T; Plakos KJI; Plaxco KW; Soh HT An Electrochemical Sensor for Single Nucleotide Polymorphism Detection in Serum Based on a Triple-Stem DNA Probe. J. Am. Chem. Soc 2009, 131, 15311–15316. [PubMed: 19807078]

(29). Venkatesan BM; Bashir R Nanopore Sensors for Nucleic Acid Analysis. Nat. Nanotechnol 2011, 6, 615–624. [PubMed: 21926981]

(30). Haff LA; Smirnov IP Single-Nucleotide Polymorphism Identification Assays Using a Thermostable DNA Polymerase and Delayed Extraction MALDI-TOF Mass Spectrometry. Genome Res. 1997, 7, 378–388. [PubMed: 9110177]

(31). Nairz K; Stocker H; Schindelholz B; Hafen E High-Resolution SNP Mapping by Denaturing HPLC. Proct. Natl. Acad. Sci. U. S. A 2002, 99, 10575–10580.

(32). Kim J; Rim YS; Chen H; Cao HH; Nakatsuka N; Hinton HL; Zhao C; Andrews AM; Yang Y; Weiss PS Fabrication of High-Performance Ultrathin $In_2O_3$ Film Field-Effect Transistors and Biosensors Using Chemical Lift-Off Lithography. ACS Nano 2015, 9, 4572–4582. [PubMed: 25798751]

(33). Nakatsuka N; Yang K-A; Abendroth JM; Cheung KM; Xu X; Yang H; Zhao C; Zhu B; Rim YS; Yang Y; Weiss PS; Stojanović MN; Andrews AM Aptamer–Field-Effect Transistors Overcome Debye Length Limitations for Small-Molecule Sensing. Science 2018, 362, 319–324. [PubMed: 30190311]

(34). Schöning MJ; Poghossian A Recent Advances in Biologically Sensitive Field-Effect Transistors (BioFETs). Analyst 2002, 127, 1137–1151. [PubMed: 12375833]

(35). Allen BL; Kichambare PD; Star A Carbon Nanotube Field-Effect-Transistor-Based Biosensors. Adv. Mater 2007, 19, 1439–1451.

(36). Curreli M; Zhang R; Ishikawa FN; Chang H; Cote RJ; Zhou C; Thompson ME Real-Time, Label-Free Detection of Biological Entities Using Nanowire-Based FETs. IEEE Trans. Nanotechnol 2008, 7, 651–667.

(37). So H-M; Won K; Kim YH; Kim B-K; Ryu BH; Na PS; Kim H; Lee J-O Single-Walled Carbon Nanotube Biosensors Using Aptamers as Molecular Recognition Elements. J. Am. Chem. Soc 2005, 127, 11906–11907. [PubMed: 16117506]

(38). Green NS; Norton ML Interactions of DNA with Graphene and Sensing Applications of Graphene Field-Effect Transistor Devices: A Review. Anal. Chim. Acta 2015, 853, 127–142. [PubMed: 25467454]

(39). Lung Khung Y; Narducci D Synergizing Nucleic Acid Aptamers with 1-Dimensional Nanostructures as Label-Free Field-Effect Transistor Biosensors. Biosens. Bioelectron 2013, 50, 278–293. [PubMed: 23872609]

(40). Cheung KM; Yang K-A; Nakatsuka N; Zhao C; Ye M; Jung ME; Yang H; Weiss PS; Stojanović MN; Andrews AM Phenylalanine Monitoring via Aptamer-Field-Effect Transistor Sensors. ACS Sensors 2019, 4, 3308–3317. [PubMed: 31631652]

(41). Chen T-Y; Loan PTK; Hsu C-L; Lee Y-H; Tse-Wei Wang J; Wei K-H; Lin C-T; Li L-J Label-Free Detection of DNA Hybridization Using Transistors Based on CVD Grown Graphene. Biosens. Bioelectron 2013, 41, 103–109. [PubMed: 22944023]

(42). Chen C-P; Ganguly A; Lu C-Y; Chen T-Y; Kuo C-C; Chen R-S; Tu W-H; Fischer WB; Chen K-H; Chen L-C Ultrasensitive in Situ Label-Free DNA Detection Using a GaN Nanowire-Based Extended-Gate Field-Effect-Transistor Sensor. Anal. Chem 2011, 83, 1938–1943. [PubMed: 21351780]

(43). Star A; Gabriel J-CP; Bradley K; Grüner G Electronic Detection of Specific Protein Binding Using Nanotube FET Devices. Nano Lett. 2003, 3, 459–463.

(44). Kim D-J; Sohn IY; Jung J-H; Yoon OJ; Lee NE; Park J-S Reduced Graphene Oxide Field-Effect Transistor for Label-Free Femtomolar Protein Detection. Biosens. Bioelectron 2013, 41, 621–626. [PubMed: 23107386]

(45). Seo G; Lee G; Kim MJ; Baek S-H; Choi M; Ku KB; Lee C-S; Jun S; Park D; Kim HG; Kim S-J; Lee J-O; Kim BT; Park EC; Kim SI Rapid Detection of COVID-19 Causative Virus (SARS-CoV-2) in Human Nasopharyngeal Swab Specimens Using Field-Effect Transistor-Based Biosensor. ACS Nano 2020, 14, 5135–5142.

(46). Humble E; Thorne MAS; Forcada J; Hoffman JI Transcriptomic SNP Discovery for Custom Genotyping Arrays: Impacts of Sequence Data, SNP Calling Method and Genotyping Technology on the Probability of Validation Success. BMC Res. Notes 2016, 9, 418. [PubMed: 27562535]

(47). Zhao C; Xu X; Bae S-H; Yang Q; Liu W; Belling JN; Cheung KM; Rim YS; Yang Y; Andrews AM; Weiss PS Large-Area, Ultrathin Metal-Oxide Semiconductor Nanoribbon Arrays Fabricated by Chemical Lift-Off Lithography. Nano Lett. 2018, 18, 5590–5595. [PubMed: 30060654]

(48). Chen H; Rim YS; Wang IC; Li C; Zhu B; Sun M; Goorsky MS; He X; Yang Y Quasi-Two-Dimensional Metal Oxide Semiconductors Based Ultrasensitive Potentiometric Biosensors. ACS Nano 2017, 11, 4710–4718. [PubMed: 28430412]

(49). Ishikawa FN; Curreli M; Chang H-K; Chen P-C; Zhang R; Cote RJ; Thompson ME; Zhou C A Calibration Method for Nanowire Biosensors to Suppress Device-to-Device Variation. ACS Nano 2009, 3, 3969–3976. [PubMed: 19921812]

(50). Pan S; Sun X; Lee JK DNA Stability in the Gas *versus* Solution Phases: A Systematic Study of Thirty-One Duplexes with Varying Length, Sequence, and Charge Level. J. Am. Soc. Mass. Spectrom 2006, 17, 1383–1395. [PubMed: 16914323]

(51). Sim A. Y. L. a. L., Jan and Herschlag, Daniel and Doniach, Sebastian. Salt Dependence of the Radius of Gyration and Flexibility of Single-Stranded DNA in Solution Probed by Small-Angle X-Ray Scattering. Phys. Rev. E 2012, 86, 021901.

(52). Weiss PS; Trevor PL; Cardillo MJ Gas–Surface Interactions on InP Monitored by Changes in Substrate Electronic Properties. J. Chem. Phys 1989, 90, 5146–5153.

(53). Cao HH; Nakatsuka N; Serino AC; Liao W-S; Cheunkar S; Yang H; Weiss PS; Andrews AM Controlled DNA Patterning by Chemical Lift-Off Lithography: Matrix Matters. ACS Nano 2015, 9, 11439–11454. [PubMed: 26426585]

(54). Howley PM; Israel MA; Law MF; Martin MA A Rapid Method for Detecting and Mapping Homology Between Heterologous DNAs. Evaluation of Polyomavirus Genomes. J. Biol. Chem 1979, 254, 4876–4883. [PubMed: 220264]

(55). Wallace RB; Shaffer J; Murphy RF; Bonner J; Hirose T; Itakura K Hybridization of Synthetic Oligodeoxyribonucleotides to Φ X 174 DNA: The Effect of Single Base Pair Mismatch. Nucleic Acids Res. 1979, 6, 3543–3558. [PubMed: 158748]

(56). Stemer DM; Abendroth JM; Cheung KM; Ye M; El Hadri MS; Fullerton EE; Weiss PS Differential Charging in Photoemission from Mercurated DNA Monolayers on Ferromagnetic Films. Nano Lett. 2020, 20, 1218–1225.

(57). Davis RR; Shaban NM; Perrino FW; Hollis T Crystal Structure of RNA-DNA Duplex Provides Insight into Conformational Changes Induced by RNase H Binding. Cell Cycle 2015, 14, 668–673. [PubMed: 25664393]

(58). Ingebrandt S; Offenhäusser A Label-Free Detection of DNA Using Field-Effect Transistors. Phys. Status Solidi A 2006, 203, 3399–3411.

(59). Liao W-S; Cheunkar S; Cao HH; Bednar HR; Weiss PS; Andrews AM Subtractive Patterning *via* Chemical Lift-Off Lithography. Science 2012, 337, 1517–1521. [PubMed: 22997333]

(60). Slaughter LS; Cheung KM; Kaappa S; Cao HH; Yang Q; Young TD; Serino AC; Malola S; Olson JM; Link S; Häkkinen H; Andrews AM; Weiss PS Patterning of Supported Gold Monolayers via Chemical Lift-Off Lithography. Beilstein J. Nanotechnol 2017, 8, 2648–2661. [PubMed: 29259879]

(61). Xu X; Yang Q; Cheung KM; Zhao C; Wattanatorn N; Belling JN; Abendroth JM; Slaughter LS; Mirkin CA; Andrews AM; Weiss PS Polymer-Pen Chemical Lift-Off Lithography. Nano Lett. 2017, 17, 3302–3311. [PubMed: 28409640]

(62). He G; Li J; Qi C; Guo X Single Nucleotide Polymorphism Genotyping in Single-Molecule Electronic Circuits. Adv. Sci 2017, 4, 1700158.

(63). Nabel CS; Manning SA; Kohli RM The Curious Chemical Biology of Cytosine: Deamination, Methylation, and Oxidation as Modulators of Genomic Potential. ACS Chem. Biol 2012, 7, 20–30. [PubMed: 22004246]

(64). Cai B; Wang S; Huang L; Ning Y; Zhang Z; Zhang G-J Ultrasensitive Label-Free Detection of PNA–DNA Hybridization by Reduced Graphene Oxide Field-Effect Transistor Biosensor. ACS Nano 2014, 8, 2632–2638. [PubMed: 24528470]

(65). Kaisti M; Kerko A; Aarikka E; Saviranta P; Boeva Z; Soukka T; Lehmusvuori A Real-Time Wash-Free Detection of Unlabeled PNA-DNA Hybridization using Discrete FET Sensor. Sci. Rep 2017, 7, 15734. [PubMed: 29147003]

(66). Hwang MT; Landon PB; Lee J; Choi D; Mo AH; Glinsky G; Lal R Highly Specific SNP Detection Using 2D Graphene Electronics and DNA Strand Displacement. Proct. Natl. Acad. Sci. U. S. A 2016, 113, 7088–7093.

(67). Kim D-S; Jeong Y-T; Park H-J; Shin J-K; Choi P; Lee J-H; Lim G An FET-Type Charge Sensor for Highly Sensitive Detection of DNA Sequence. Biosens. Bioelectron 2004, 20, 69–74. [PubMed: 15142578]

(68). Kergoat L; Piro B; Berggren M; Pham M-C; Yassar A; Horowitz G DNA Detection with a Water-Gated Organic Field-Effect Transistor. Org. Electron 2012, 13, 1–6.

(69). Uslu F; Ingebrandt S; Mayer D; Böcker-Meffert S; Odenthal M; Offenhäusser A Labelfree Fully Electronic Nucleic Acid Detection System Based on a Field-Effect Transistor Device. Biosens. Bioelectron 2004, 19, 1723–1731. [PubMed: 15142607]

(70). Lin C-H; Hung C-H; Hsiao C-Y; Lin H-C; Ko F-H; Yang Y-S Poly-Silicon Nanowire Field-Effect Transistor for Ultrasensitive and Label-Free Detection of Pathogenic Avian Influenza DNA. Biosens. Bioelectron 2009, 24, 3019–3024. [PubMed: 19362813]

(71). Sorgenfrei S; Chiu C.-y.; Gonzalez RL Jr; Yu Y-J; Kim P; Nuckolls C; Shepard KL Label-Free Single-Molecule Detection of DNA-Hybridization Kinetics With a Carbon Nanotube Field-Effect Transistor. Nat. Nanotechnol 2011, 6, 126–132. [PubMed: 21258331]

(72). Xu S; Zhan J; Man B; Jiang S; Yue W; Gao S; Guo C; Liu H; Li Z; Wang J; Zhou Y Real-Time Reliable Determination of Binding Kinetics of DNA Hybridization Using a Multi-Channel Graphene Biosensor. Nat. Commun 2017, 8, 14902. [PubMed: 28322227]

(73). Stine R; Robinson JT; Sheehan PE; Tamanaha CR Real-Time DNA Detection Using Reduced Graphene Oxide Field Effect Transistors. Adv. Mater 2010, 22, 5297–5300. [PubMed: 20872408]

(74). Hwang MT; Wang Z; Ping J; Ban DK; Shiah ZC; Antonschmidt L; Lee J; Liu Y; Karkisaval AG; Johnson ATC; Fan C; Glinsky G; Lal R DNA Nanotweezers and Graphene Transistor Enable Label-Free Genotyping. Adv. Mater 2018, 30, 1802440.

(75). Ping J; Vishnubhotla R; Vrudhula A; Johnson ATC Scalable Production of High-Sensitivity, Label-Free DNA Biosensors Based on Back-Gated Graphene Field Effect Transistors. ACS Nano 2016, 10, 8700–8704. [PubMed: 27532480]

(76). Xie P; Xiong Q; Fang Y; Qing Q; Lieber CM Local Electrical Potential Setection of DNA by Nanowire–Nanopore Sensors. Nat. Nanotechnol 2011, 7, 119–125. [PubMed: 22157724]

(77). Reina G; González-Domínguez JM; Criado A; Vázquez E; Bianco A; Prato M Promises, Facts and Challenges for Graphene in Biomedical Applications. Chem. Soc. Rev 2017, 46, 4400–4416. [PubMed: 28722038]

(78). Yan L; Zheng YB; Zhao F; Li S; Gao X; Xu B; Weiss PS; Zhao Y Chemistry and Physics of a Single Atomic Layer: Strategies and Challenges for Functionalization of Graphene and Graphene-Based Materials. Chem. Soc. Rev 2012, 41, 97–114. [PubMed: 22086617]

(79). Cheung KM; Stemer DM; Zhao C; Young TD; Belling JN; Andrews AM; Weiss PS Chemical Lift-Off Lithography of Metal and Semiconductor Surfaces. ACS Mat. Lett 2020, 2, 76–83.

(80). Belling JN; Cheung KM; Jackman JA; Sut TN; Allen M; Park JH; Jonas SJ; Cho N-J; Weiss PS Lipid Bicelle Micropatterning Using Chemical Lift-Off Lithography. ACS Appl. Mater. Interfaces 2020, 12, 13447–13455.

(81). Price CP; Kricka LJ Improving Healthcare Accessibility Through Point-of-Care Technologies. Clin. Chem 2007, 53, 1665–1675. [PubMed: 17660275]

(82). Kim HS; Byrne PD; Facchetti A; Marks TJ High Performance Solution-Processed Indium Oxide Thin-Film Transistors. J. Am. Chem. Soc 2008, 130, 12580–12581. [PubMed: 18759390]

(83). Curreli M; Li C; Sun Y; Lei B; Gundersen MA; Thompson ME; Zhou C Selective Functionalization of $In_2O_3$ Nanowire Mat Devices for Biosensing Applications. J. Am. Chem. Soc 2005, 127, 6922–6923. [PubMed: 15884914]

(84). Rim YS; Bae S-H; Chen H; Yang JL; Kim J; Andrews AM; Weiss PS; Yang Y; Tseng H-R Printable Ultrathin Metal Oxide Semiconductor-Based Conformal Biosensors. ACS Nano 2015, 9, 12174–12181. [PubMed: 26498319]

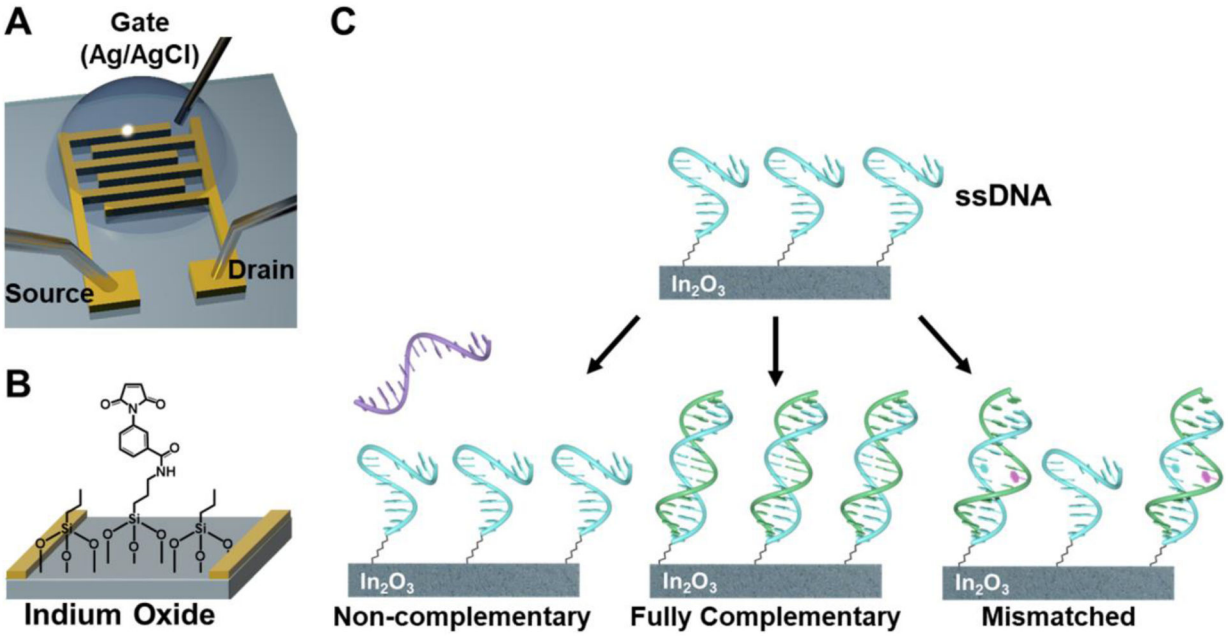


**Figure 1. Oligonucleotide detection *via* field effect transistors (FETs).**

**(A)** Transistors ($2 \times 3$ mm$^2$) were composed of 4-nm thin-film $In_2O_3$ as the channel material, with 10-nm Ti adhesion and 30-nm top Au layers patterned as interdigitated electrodes. The FETs were operated in a solution-gated setup with a Ag/AgCl reference electrode as the gate electrode. **(B)** Thiolated single-stranded DNA (ssDNA) was tethered to amine-terminated silanes co-assembled with methyl-terminated silanes on metal oxide surfaces using *m*-maleimidobenzoyl-*N*-hydroxysuccinimide ester as a linker. **(C)** Field-effect transistors functionalized with ssDNA were exposed to non-complementary, fully complementary, or mismatched sequences.

A

| | |
|---|---|
| Thiolated: | HS–GGT TCT TGG ATA TAG |
| Complementary: | CCA AGA ACC TAT ATC |
| Non-complementary: | TAA ATC ACA CTG CAC |

B

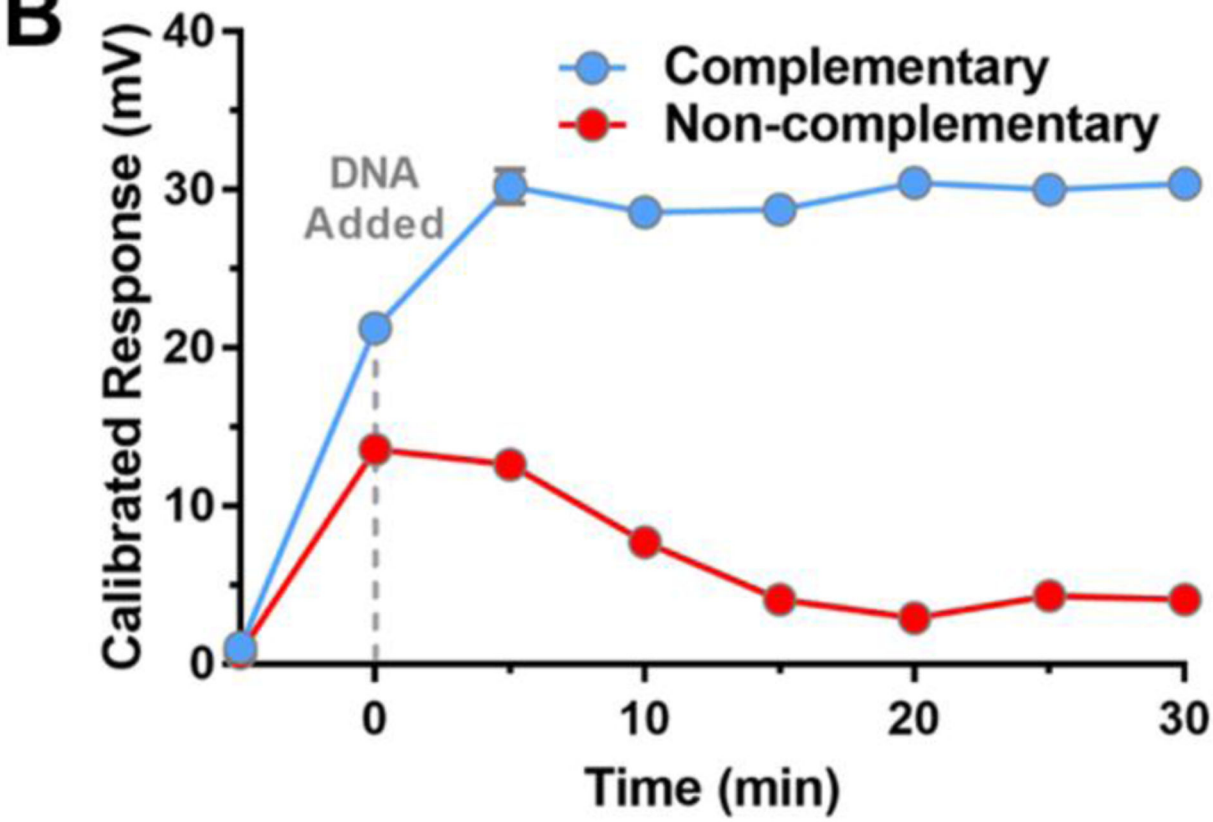


**Figure 2. Temporal response of field-effect transistors (FETs) to DNA hybridization.**

**(A)** Sequences of DNA for FET measurements. **(B)** Responses of two representative FETs with respect to incubation time with solutions containing either fully complementary or non-complementary sequences. The DNA solutions were added to FETs at 0 min. Responses associated with complementary sequences remained elevated, while responses to non-complementary sequences showed initial increases followed by decreases in conductance ultimately resulting in negligible changes in FET calibrated responses. Error bars, which are too small to be visualized in some cases, are standard errors of the means for $N$=5 consecutive gate-voltage sweeps at each time point.

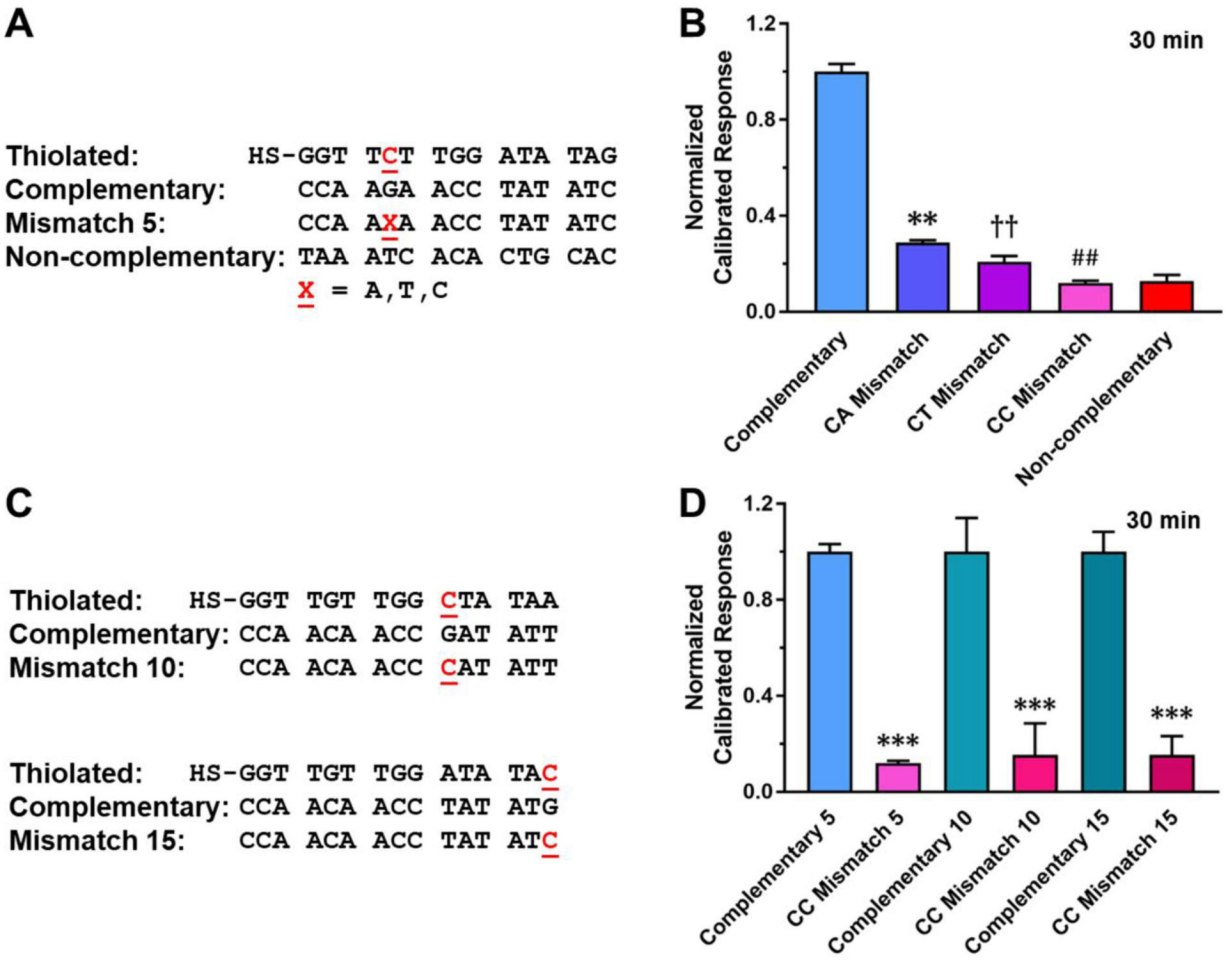


**Figure 3. Discrimination of single nucleotide variations.**

**(A)** Sequences of DNA used for field-effect transistor (FET) measurements with different types of mismatches at the 5$^{th}$ position from the attachment location. **(B)** Mean field-effect transistor (FET) responses after 30 min of target DNA exposure demonstrating discrimination of sequences with single base-pair mismatches. Error bars are standard errors of the means with $N$=3 FETs/group. ** $P$<0.01 *vs* complementary, CT, CC, and non-complementary, †† $P$<0.01 *vs* complementary, CA, CC, and non-complementary, ## $P$<0.01 *vs* complementary, CA, and CT. **(C)** Sequences of DNA for FET measurements with the same mismatch at the 10$^{th}$ or 15$^{th}$ position from the attachment location. **(D)** Mean FET responses after 30 min of target DNA incubation differentiating sequences with a CC mismatch at the 5$^{th}$, 10$^{th}$, or 15$^{th}$ position. Error bars are standard errors of the means with $N$=3 FETs/group. *** $P$<0.001 *vs* the corresponding fully complementary DNA. Data for complementary and CC mismatched sequences at the 5$^{th}$ position are reproduced from (B) for comparison.

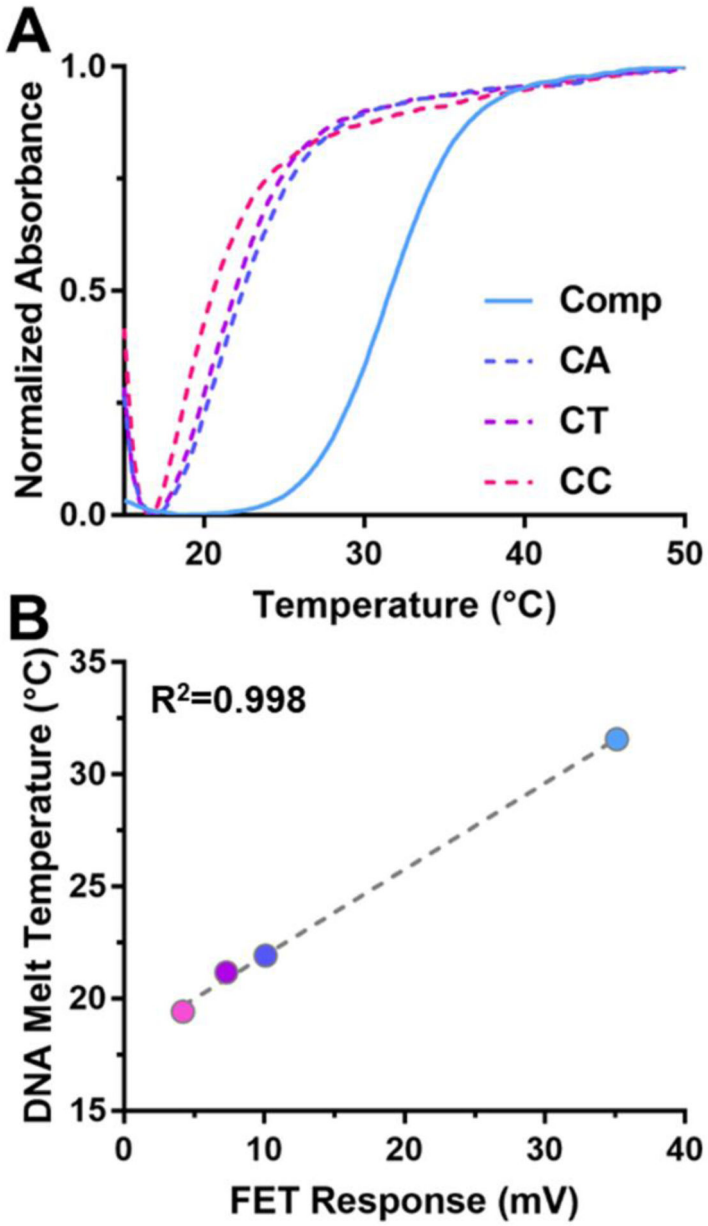


**Figure 4. DNA melt-curve analysis.**

**(A)** DNA melting curves for dehybridization of sequences in Figure 3A showing relative stabilities of different mismatches *vs* fully complementary hybridization. **(B)** Correlation of field-effect transistor (FET) calibrated responses to different sequences from Figure 3B *vs* melting temperatures. The linearity index ($R^2$) is indicated. Symbol colors are as defined in (A).

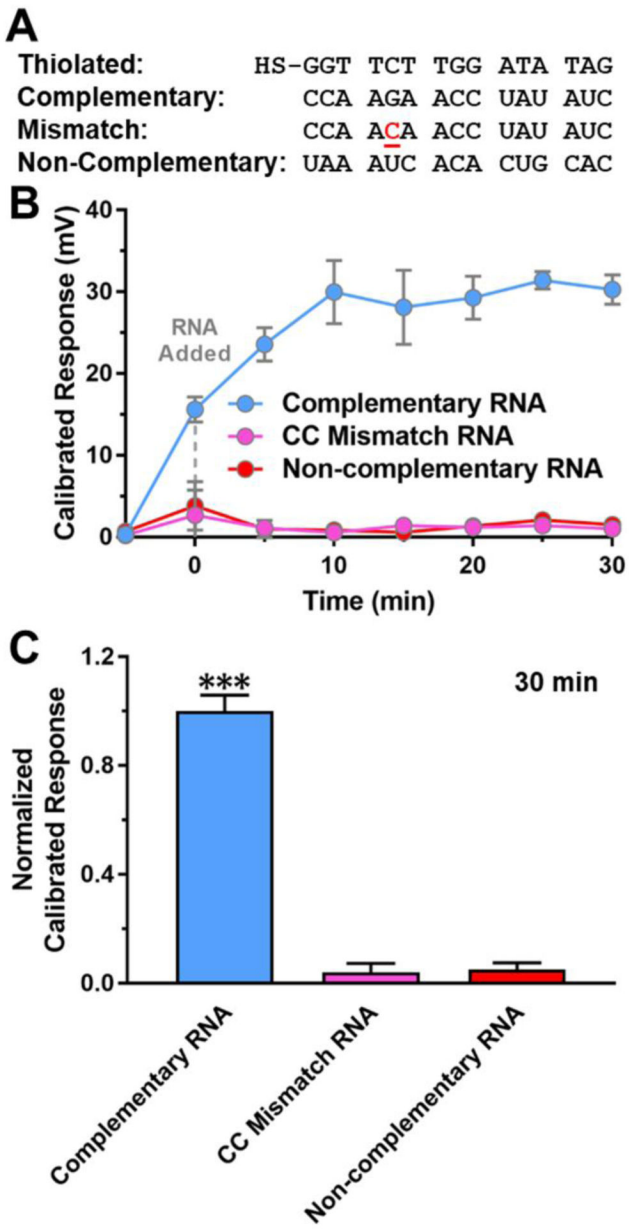


**Figure 5. Sequence-specific RNA detection.**

**(A)** Sequences of RNA used for field-effect transistor (FET) measurements. **(B)** Representative DNA-functionalized field-effect transistor (FET) responses with respect to time after incubation with RNA. Calibrated responses to complementary sequences increased and remained stable over time while responses to non-complementary and mismatched sequences were negligible. Error bars, which are too small to be visualized in some cases, are standard errors of the means for $N$=5 consecutive gate-voltage sweeps at each time point for a single representative FET per condition. **(C)** Mean FET responses after 30 min of RNA incubation demonstrating differentiation of complementary RNA *vs* CC

mismatched and non-complementary RNA. Error bars are standard errors of the means with $N$=2 FETs/group. *** $P$<0.001 *vs* CC mismatch and non-complementary RNA.